Supporting Information

Metformin reprogram tumor microenvironment and boost chemoimmunotherapy in colorectal cancer

Weidong Ni[1,2], Jiayan Wu[1], Yuanji Feng[1], Yingying Hu[1], Haiyan Liu[3], Jie Chen[1]*, Fangfang Chen[2]*, Huayu Tian[1]*

[1]Key Laboratory of Polymer Ecomaterials, Changchun Institute of Applied Chemistry Chinese Academy of Sciences, Changchun 130022, PR China

[2]Key Laboratory of Pathobiology, Ministry of Education, Nanomedicine and Translational Research Center, China-Japan Union Hospital of Jilin University, Changchun 130033, PR China

[3]Center for Biological Experiment, College of Basic Medicine, Jilin University, Changchun 130021, PR China.

*Corresponding author: chenjie@ciac.ac.cn (J. Chen); cff@jlu.edu.cn (F. Chen); thy@xmu.edu.cn (H. Tian)

Supporting Figures

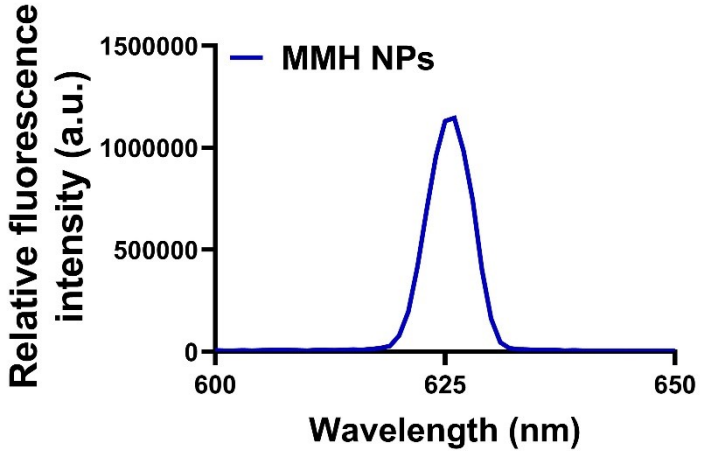

Fig. S1 The Fluorescence spectra curve of MMH NPs.

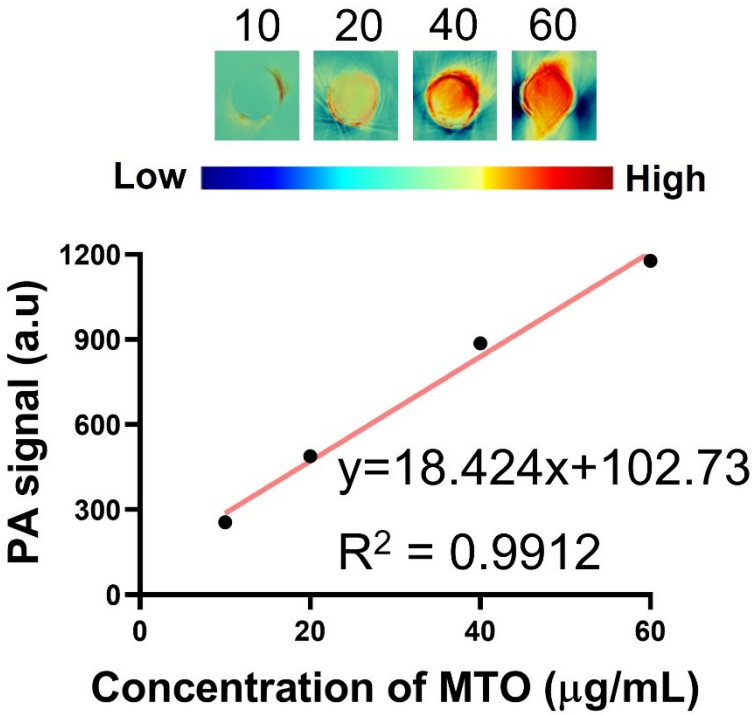

Fig. S2 Plots of photoacoustic values of MMH NPs and corresponding PA imaging at varying concentrations.

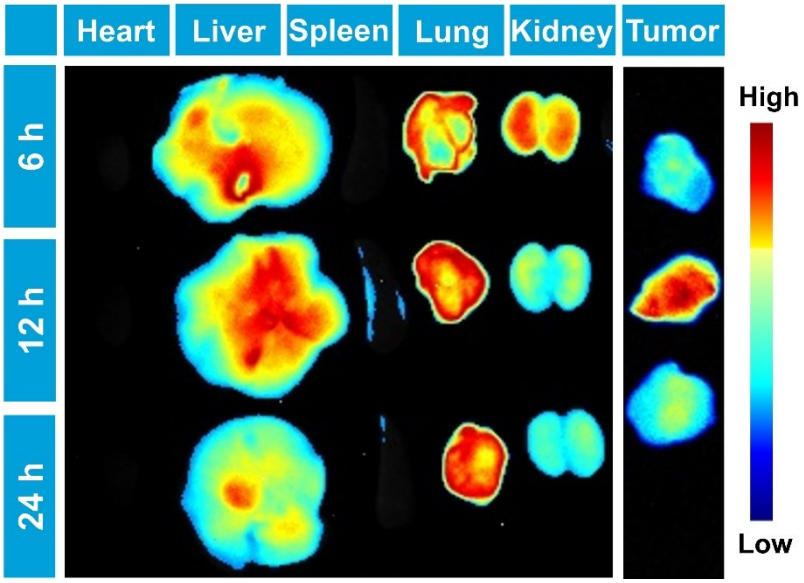

Fig. S3 Biodistribution of the MMH NPs in organs (heart, liver, spleen, lung, and kidney) and tumor at 6, 12, and 24 h post-injection.

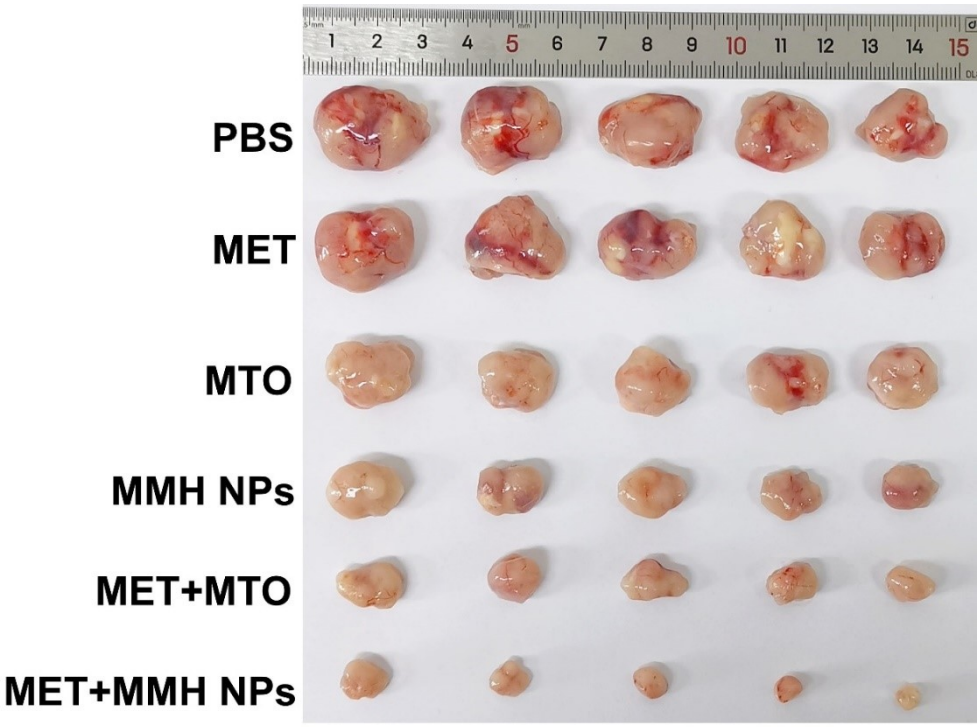

Fig. S4 The tumor photos after the different treatments on day 21.

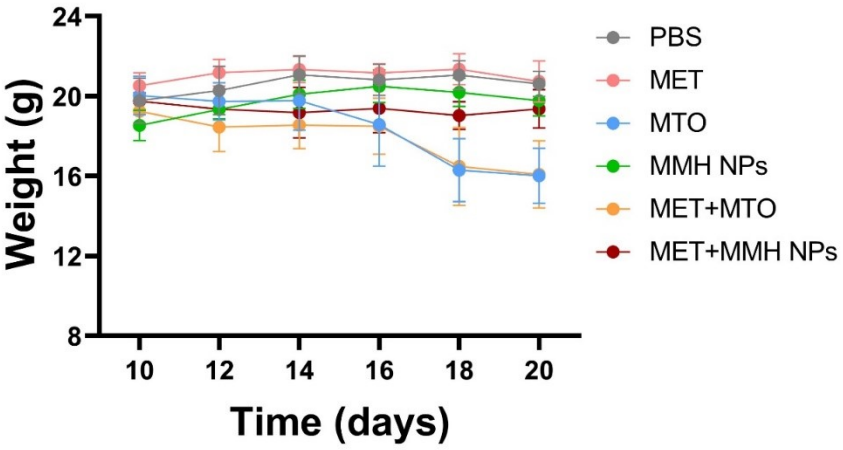

Fig. S5 The body weight of Balb/c tumor-bearing mice after the different treatments.

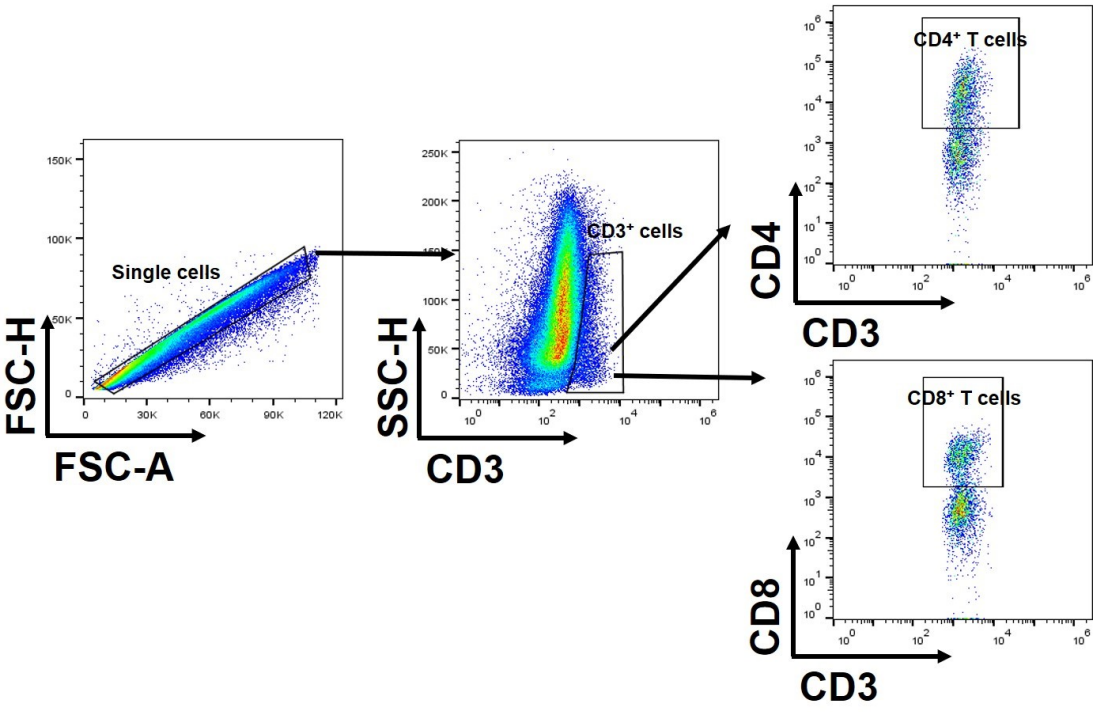

Fig. S6 The gating strategy for $CD4^+$ and $CD8^+$ T cells analysis in the subcutaneous tumor.

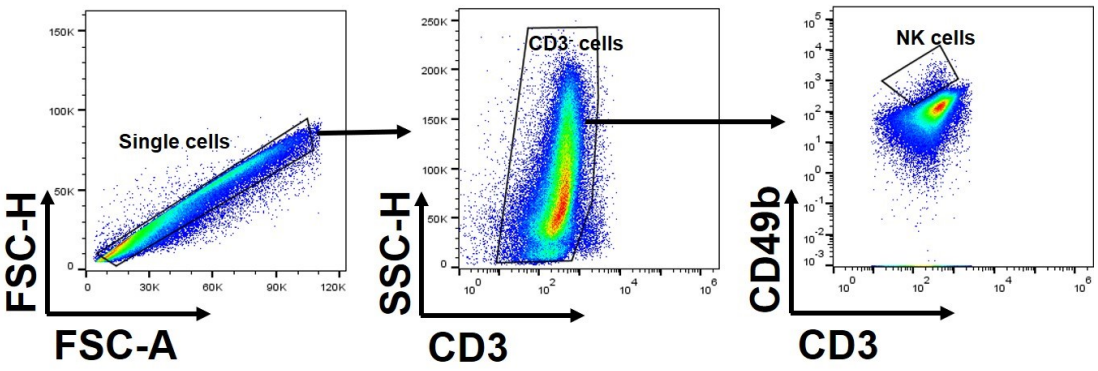

Fig. S7 The gating strategy for NK cells analysis in the subcutaneous tumor.

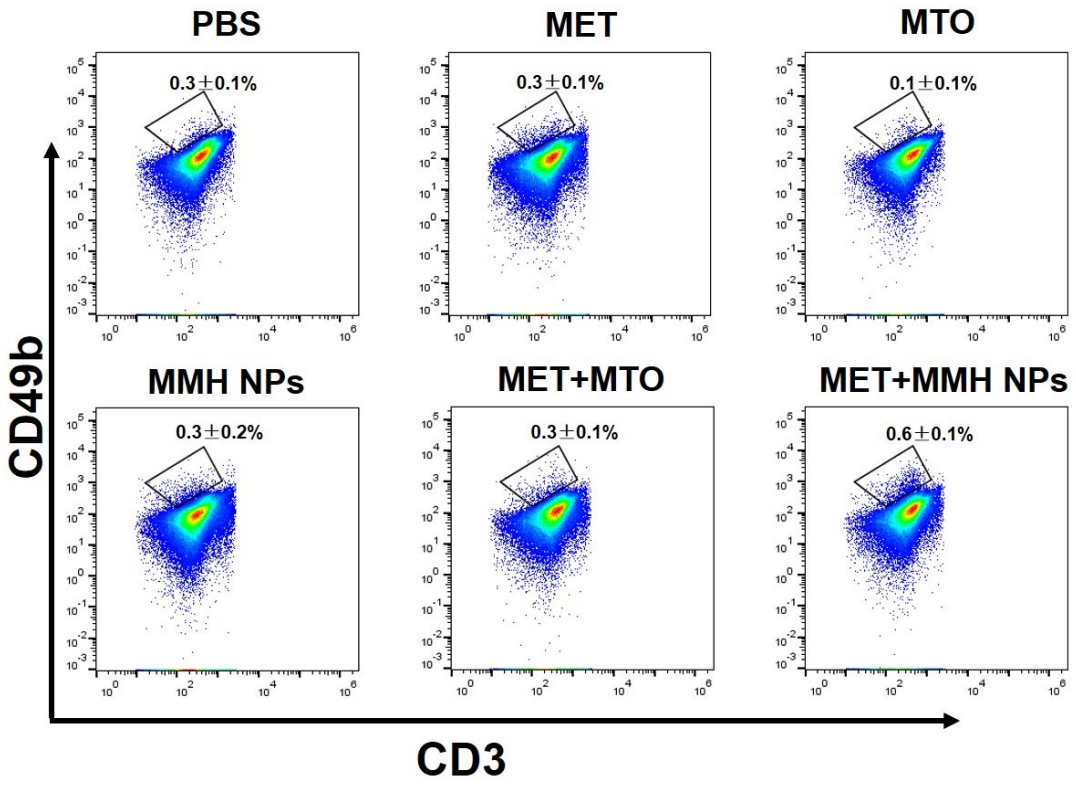

Fig. S8 The representative flow cytometric quantification of infiltrating NK cells in the tumor.

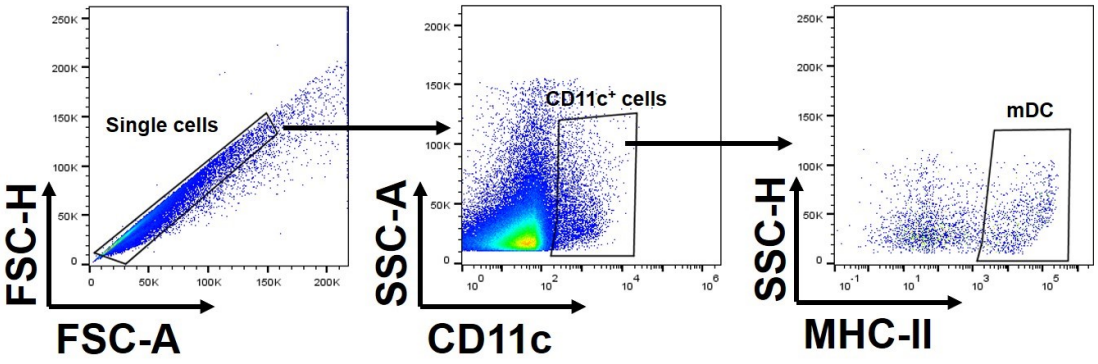

Fig. S9 The gating strategy for mature DCs analysis in the TDLNs.

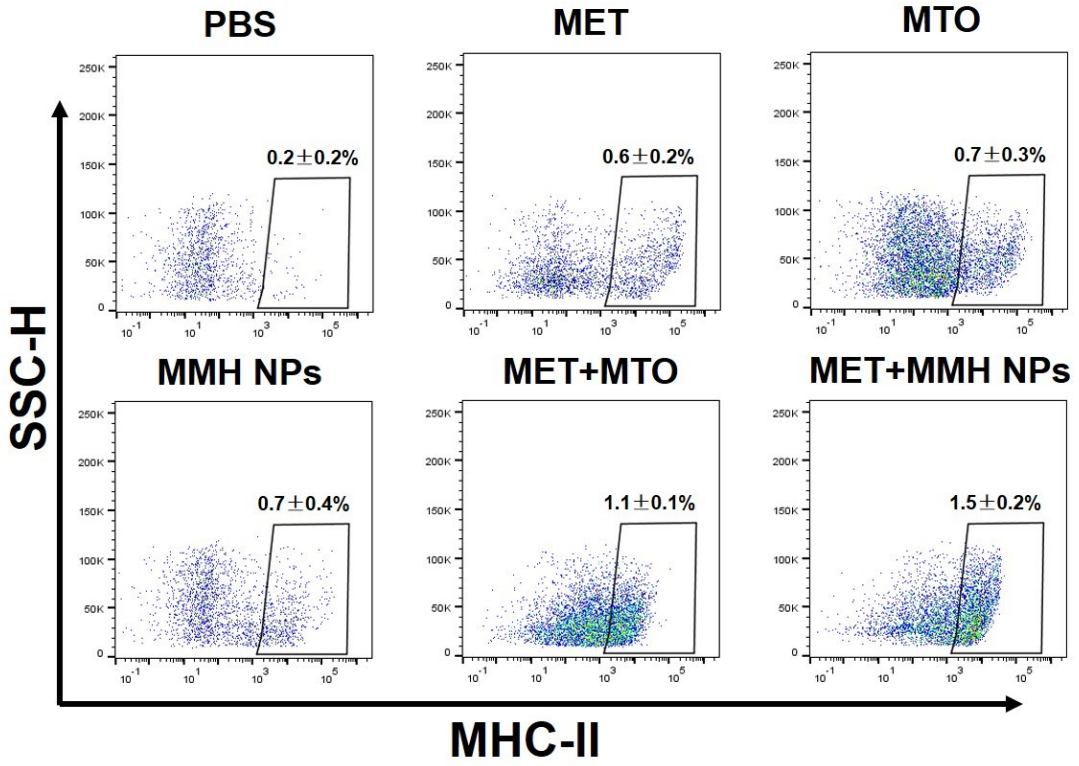

Fig. S10 The representative flow cytometric quantification of infiltrating mature DCs in the TDLNs.

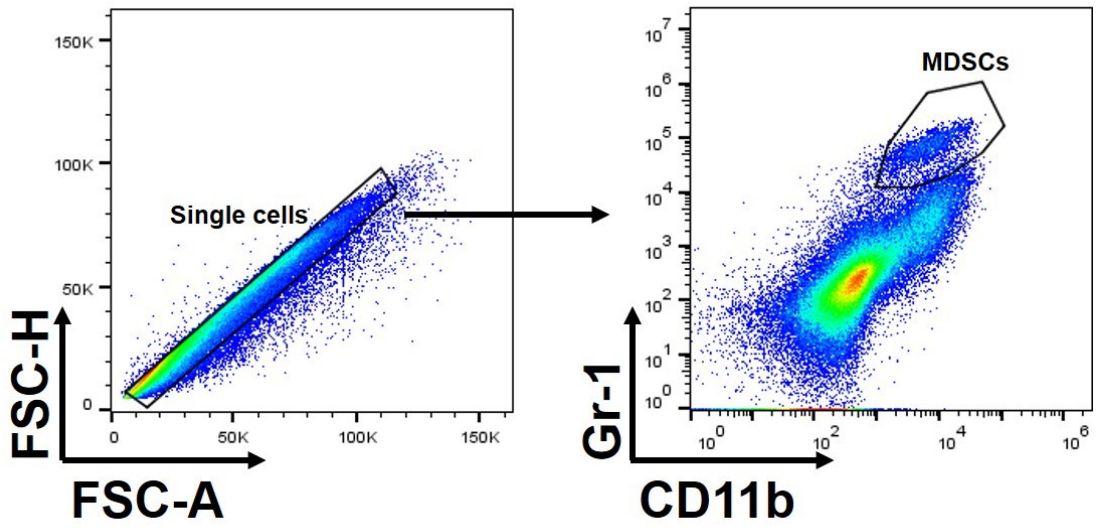

Fig. S11 The gating strategy for MDSCs in the subcutaneous tumor.

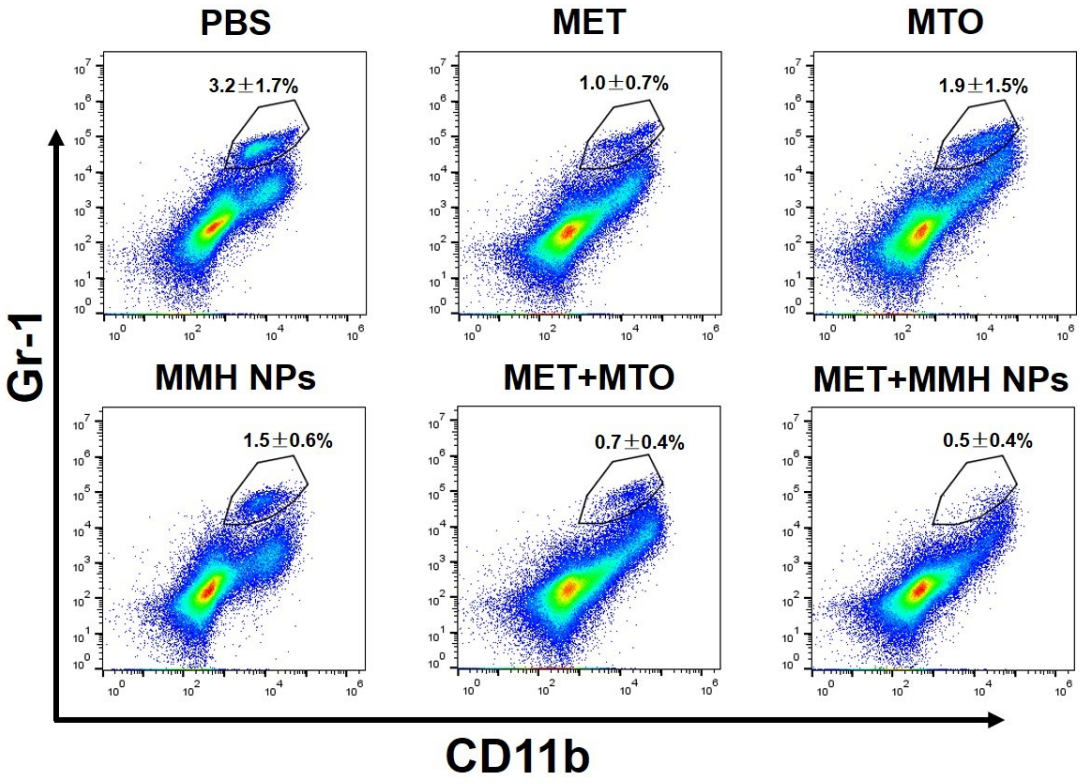

Fig. S12 The representative flow cytometric quantification of infiltrating MDSCs in the tumor.

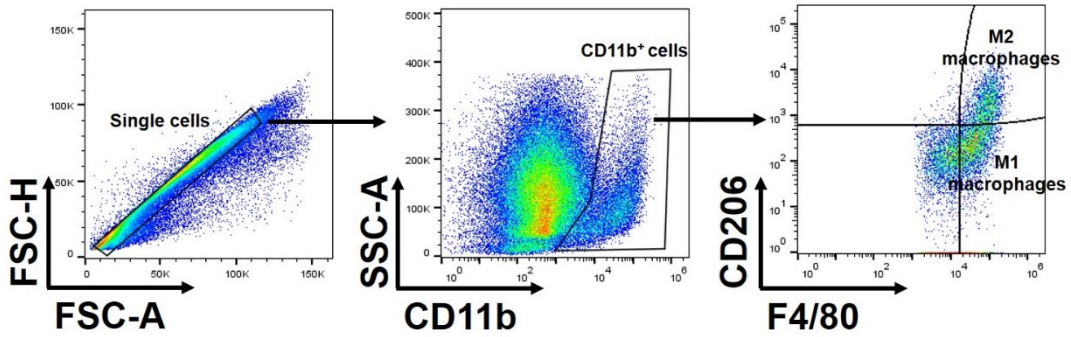

Fig. S13 The gating strategy for M2 and M1 macrophages in the subcutaneous tumor.

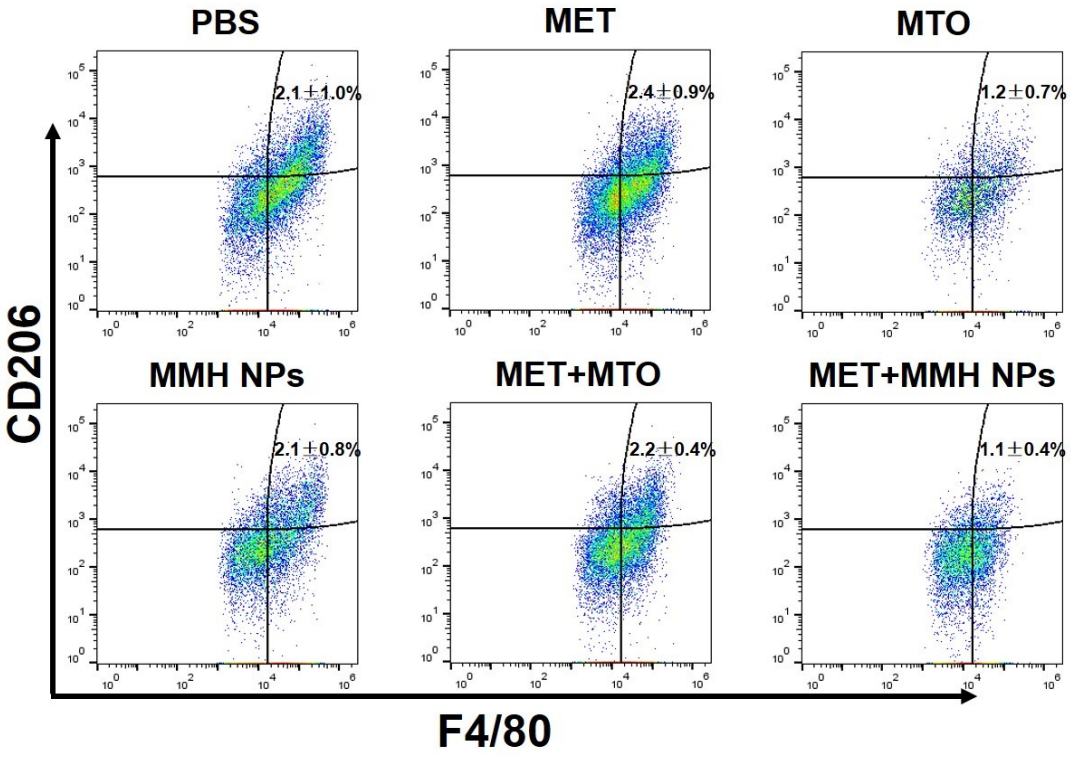

Fig. S14 The representative flow cytometric quantification of infiltrating M2 macrophages in the tumor.

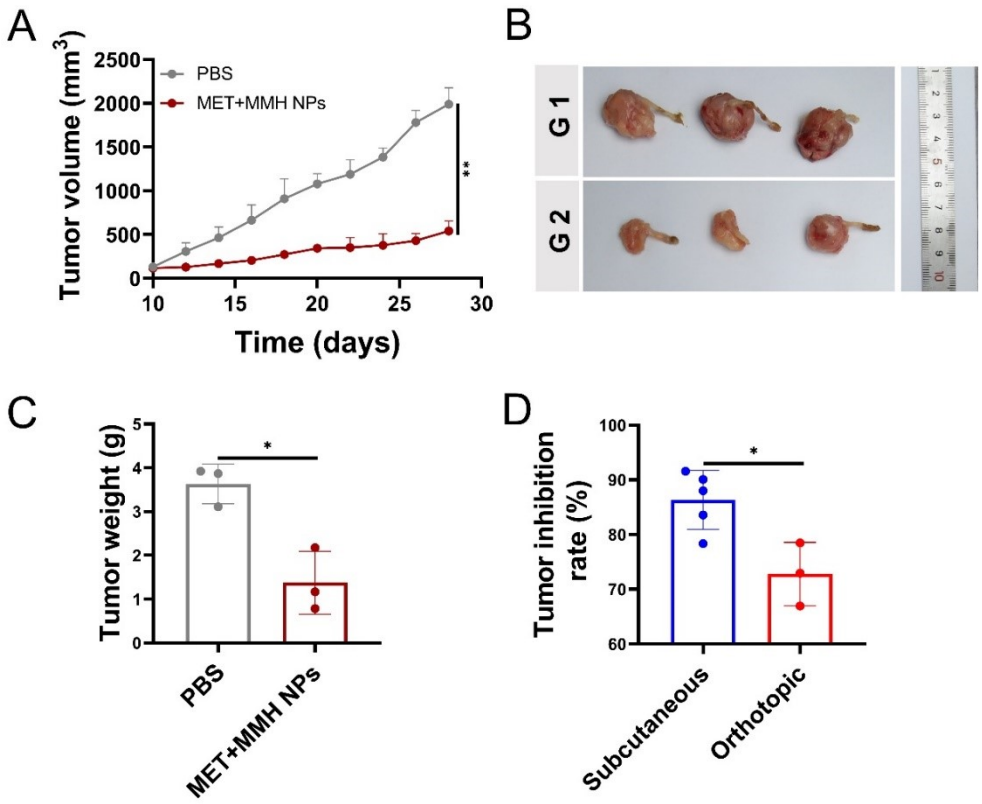

Fig. S15 In vivo antitumor effect was assessed in the orthotopic CRC tumor-bearing mice model. (A) The average tumor growth curves of orthotopic CRC tumor-bearing mice in different groups. The tumor image (B) and average tumor weight (C) of orthotopic tumors after different treatments. G1, PBS; G2, MET+MMH NPs. (D) The average tumor growth volume inhibitory rate of MET+MMH NPs group in a subcutaneous and orthotopic tumor.

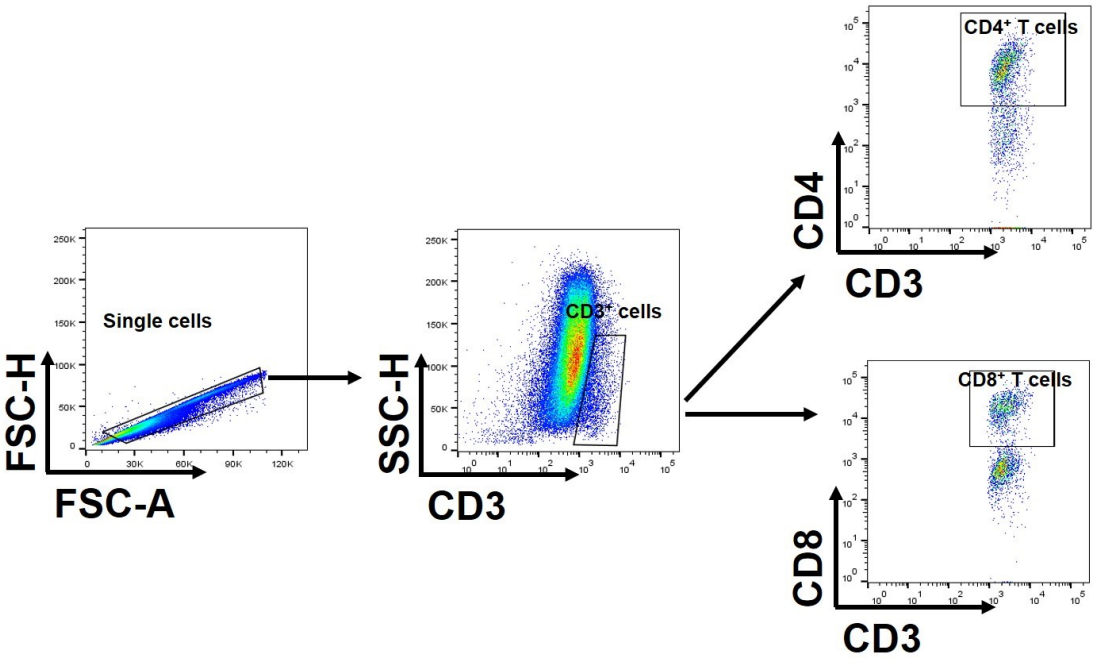

Fig. S16 The gating strategy for $CD4^+$ and $CD8^+$ T cells analysis in the orthotopic tumor.

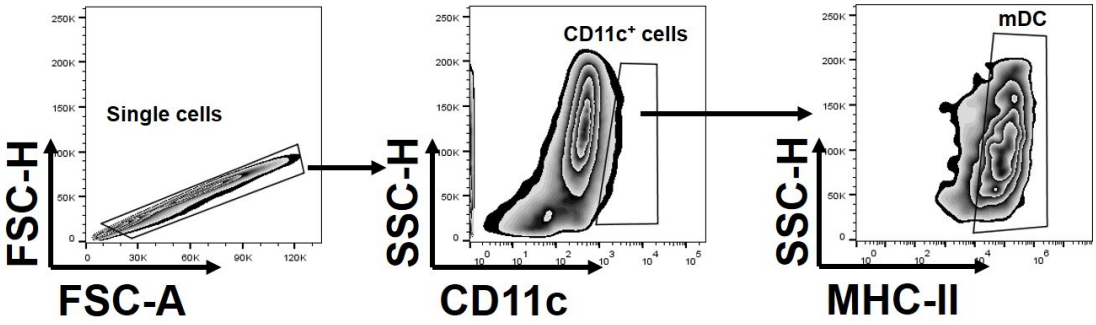

Fig. S17 The gating strategy for mature DCs analysis in the orthotopic tumor.

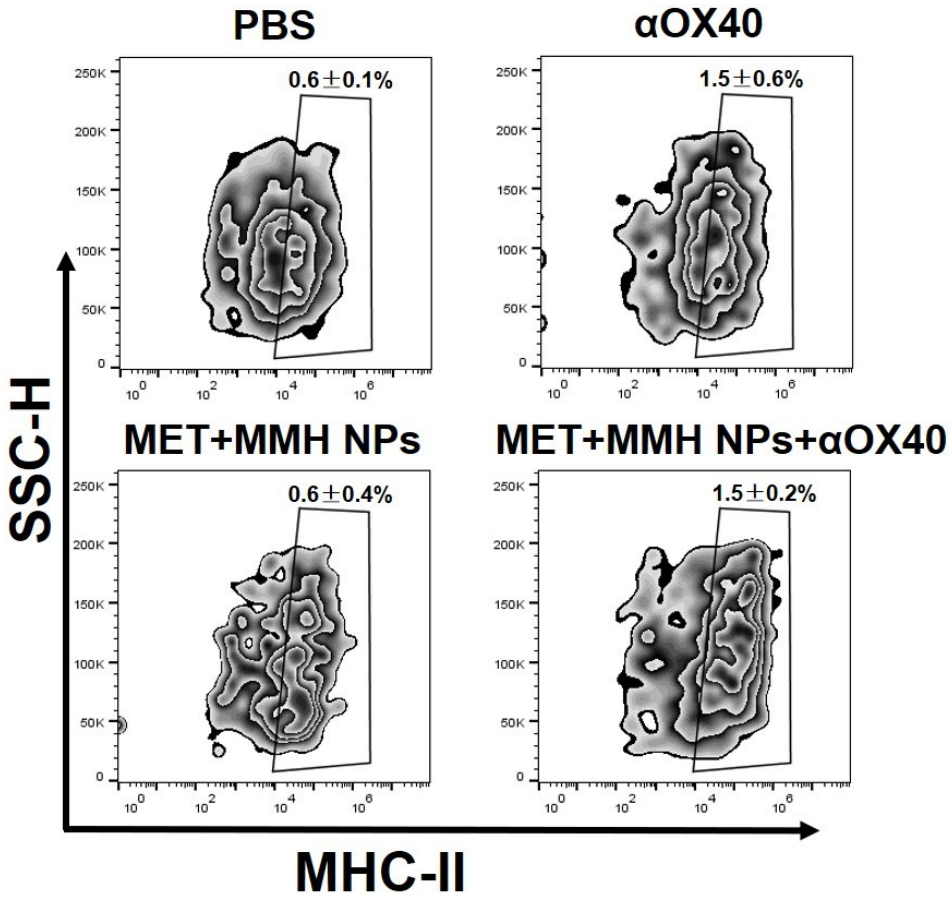

Fig. S18 The representative flow cytometric quantification of infiltrating mDCs in the orthotopic CRC.

Table S1 Antibodies were used for flow cytometry, IF or IHC in this study.

Antibodies	Company	Catalog No.	Application	Dilution
Anti-CD45 (APC-Cy7)	BioLegend	157204	Flow	1:250
Anti-CD3 (FITC)	BioLegend	100203	Flow	1:250
Anti-CD4 (PE-Cy7)	BioLegend	100422	Flow	1:250
Anti-CD8a (APC)	BioLegend	100712	Flow	1:250
Anti-CD49b (PE)	BioLegend	103506	Flow	1:250
Anti-CD11b (FITC)	BioLegend	101206	Flow	1:250
Anti-F4/80 (PE-Cy7)	BioLegend	123114	Flow	1:250
Anti-Gr-1 (PE)	BioLegend	108408	Flow	1:250
Anti-CD206 (BV 650)	BioLegend	141723	Flow	1:250
Anti-CD11c (FITC)	BioLegend	117306	Flow	1:250
Anti-MHC II (APC-Cy7)	BioLegend	107628	Flow	1:250
Anti-CRT	Abcam	ab2907	IF	1:50
Anti-HMGB1	Abcam	ab227168	IF	1:50
Anti-α-SMA	Servicebio	GB111364	IHC	1:100
Anti-CD31	CST	77699	IHC	1:100
Anti-CD8a	Thermo Fisher	14-0808-82	IHC	1:100

Flow: Flow cytometry. IHC: Immunohistochemistry. IF: Immunofluorescence.